IOPscience iopscience.iop.org

Home Search Collections Journals About Contact us My IOPscience

Nature of the hyper-Raman active vibrations of lithium borate glasses

This article has been downloaded from IOPscience. Please scroll down to see the full text article.

2008 J. Phys.: Condens. Matter 20 155103

(http://iopscience.iop.org/0953-8984/20/15/155103)

View the table of contents for this issue, or go to the journal homepage for more

Download details:
IP Address: 129.252.86.83
The article was downloaded on 29/05/2010 at 11:28

Please note that terms and conditions apply.

J. Phys.: Condens. Matter **20** (2008) 155103 (7pp) doi:10.1088/0953-8984/20/15/155103

Nature of the hyper-Raman active vibrations of lithium borate glasses

G Simon, B Hehlen, R Vacher and E Courtens

Laboratoire des Colloïdes, Verres et Nanomatériaux (LCVN), UMR 5587 CNRS,
University of Montpellier II, F-34095 Montpellier, France

E-mail: bernard.hehlen@lcvn.univ-montp2.fr

Received 13 November 2007, in final form 12 February 2008
Published 4 March 2008
Online at stacks.iop.org/JPhysCM/20/155103

Abstract

Hyper-Raman spectra of two lithium borate glasses, $4B_2O_3$:Li_2O and $2B_2O_3$:Li_2O, are compared to those of pure boron oxide glass, v-B_2O_3. A mode analysis is performed using a structural model based on the symmetry of the elementary structural units (ESUs) constituting the glasses. Most spectral components arise from *internal* vibrations of BO_3 triangles, B_3O_3 boroxol rings, and BO_4 tetrahedra. In particular, a mode associated with stretching motions of BO_4 units can be assigned to a vibration of F_2 symmetry in the T_d tetrahedral point group. The hyper-Raman scattering intensity of its transverse optic component appears to be proportional to the number of BO_4 units in the glass. The boson peak observed in hyper-Raman scattering arises from *external* modes of rigid ESUs which correspond to librational motions coupled to their translations. The scattering strength of these modes strongly decreases with increasing Li concentration. In pure v-B_2O_3, external modes of *boroxols* presumably dominate this scattering. The decrease in the boroxol concentration in lithium borate glasses correlates with the apparent hardening of the boson peak.

1. Introduction

On the atomic scale, oxide glasses are usually composed of well defined strongly bonded elementary structural units (ESUs). These are for example the SiO_4 tetrahedra of silica glass, v-SiO_2, or the BO_3 triangles of vitreous boron oxide, v-B_2O_3. These rather rigid ESUs are connected to each other by looser bonds with a larger distribution of distances and angles. The random connexions essentially produce the glass disorder. However, the connected ESUs can also form larger well defined structures, such as the small rings in the three prototypical glasses v-SiO_2 [1], v-GeO_2 [2, 3], and v-B_2O_3 [4–6]. In general, owing to disorder, the structure of oxide glasses beyond the second neighbors is hard to unravel by the usual structural tools.

The measurement of the vibrations by optical spectroscopies, such as infrared absorption (IR) or Raman scattering (RS), provides an alternate way to gain structural information on the local and intermediate scales. This was demonstrated long ago, e.g. through the observation of the above-mentioned ring structures in v-SiO_2. Two narrow lines appear in the Raman spectra at 495 cm^{-1} (D_1) and 609 cm^{-1} (D_2), associated with breathing motions of oxygen atoms in well defined $(-Si-O-)_n$ rings with $n = 4$ and 3, respectively [1]. The number density of these small-n rings is too small [7] to allow for their observation by structural techniques, which only give average information. Boron oxide, v-B_2O_3, also exhibits a medium range ring structure resulting from the bonding of three BO_3 triangles into a boroxol B_3O_3. The latter are flat and rigid, very close to the perfect D_{3h} symmetry. The formation of boroxol rings in B_2O_3 glass was first observed by x-ray diffraction [4]. Their abundance has been the subject of a long debate. It is only recently, with the help of NMR [8] and numerical simulations [9], that it was established beyond reasonable doubt that the numbers of B_3O_3 rings and remaining BO_3 triangles are in a ratio close to 1:1. Boroxols are easily observed in RS: the breathing motion of oxygen atoms in the rings produces a narrow polarized line at 808 cm^{-1}, which dominates the entire spectrum [6].

Apart from this last example, the nature of vibrations in borate glasses is not very well known. It is thus worthwhile to gain additional information using a different optical spectroscopy with other selection rules, namely hyper-Raman scattering (HRS) [10]. Alternatively, it would also be useful to apply impulsive stimulated Raman scattering [3, 11], as time resolution can help unraveling spectral components. In this

 © 2008 IOP Publishing Ltd Printed in the UK

paper we summarize the results of hyper-Raman spectroscopy on pure B_2O_3 and present new data for two lithium borate glasses, tetraborate $4B_2O_3$:Li_2O and diborate $2B_2O_3$:Li_2O. The remainder of the paper is organized as follows. The next section briefly describes hyper-Raman scattering and our implementation of the experiment. Section 3 summarizes previous results on pure boron oxide glass. Section 4 discusses the modes produced by internal vibrations of the ESUs in lithium borate glasses. Section 5 presents the results on the boson peak, while section 6 concludes the paper.

2. Hyper-Raman scattering experiment

Hyper-Raman scattering is a non-linear spectroscopy in which two incident photons produce one scattered photon after interaction with an excitation in the medium. It corresponds to the first non-linear term in the expansion of the *induced* dipole moment **p** as a function of the incident electric field **E**. For the structural unit m one writes

$$\mathbf{p}^m = \boldsymbol{\chi}_m^{(1)} \cdot \mathbf{E} + \tfrac{1}{2}\boldsymbol{\chi}_m^{(2)} : \mathbf{EE} + \cdots, \tag{1}$$

where $\boldsymbol{\chi}_m^{(1)}$ and $\boldsymbol{\chi}_m^{(2)}$ are the first- and second-order susceptibility tensors, respectively. The vibrations modulate the susceptibilities $\boldsymbol{\chi}$. Raman scattering is then associated with the first term in equation (1) (proportional to **E**), while it is the second term (proportional to the square of **E**) that produces HRS. The RS and HRS spectra are proportional to the Fourier transformed space and time correlation functions of the dipole moment fluctuation $\delta\mathbf{p}$ due to the vibrations and induced in the material by the incident electric field **E**. IR absorption originates from a modulation of the *permanent* dipole moment of the ESUs by the vibrations.

HRS is usually difficult to observe owing to the very weak efficiency of the scattering process, the signal being typically $\sim 10^6$ times weaker than the RS one [10]. This can now be overcome using a pulsed laser of sufficiently high power, large aperture optics, and a high sensitivity CCD camera. The design of our hyper-Raman spectrometer is described elsewhere [12]. The main interest of HRS is that the selection rules are different from those of RS and IR absorption. IR active modes are always active in HRS. However, HRS provides direct and separate information on the transverse optic (TO) and longitudinal optic (LO) components, whereas IR most often just measures the reflectivity spectrum. In the latter case, separating TO from LO is achieved via the Kramers–Kronig relation. To avoid artifacts this requires precise IR spectra covering a broad frequency range. In addition, HRS probes the bulk while IR reflectivity can be sensitive to the state of the surface. Further, there also exists modes that are inactive both in IR and RS, but that are active in HRS. This is the case for example of the librational motions of rigid SiO_4 tetrahedra in v-SiO_2, which have been well identified in HRS [13, 14]. It is such motions that contribute most to the excess of vibrational states at low frequencies, i.e. the so-called boson peak of v-SiO_2.

3. A summary of results on pure v-B_2O_3

HRS spectroscopy from boron oxide has proven to be helpful for the assignment of the vibrational modes [15, 16]. The analysis of the vibrations was performed with a very simple structural model taking into account the local symmetry of the ESUs constituting the glass, that is the BO_3 triangles and the B_3O_3 boroxol rings. Both structural units happen to belong to the same point group, D_{3h}. Hence, the ESU vibrations decompose into the following irreducible representations [17]:

$$\begin{aligned} &A_1'(\mathrm{RS, HRS}) + A_2'(\mathrm{HRS}) + A_2''(\mathrm{IR, HRS}) \\ &\quad + E'(\mathrm{IR, HRS}) + E''(\mathrm{RS, HRS}). \end{aligned} \tag{2}$$

The activity of modes in the optical spectroscopies is given in parentheses.

Our sample was prepared from isotopically pure (99.6%) $^{11}B_2O_3$ powder containing $\sim$1 wt% moisture. After preparation, which involved a dehydration process, a water content of $\sim$0.8 wt% was determined by measuring the infrared transmission of a thin slice [18]. Figure 1 shows the HRS VV spectrum (figure 1(a)) and the RS VV spectrum (figure 1(b)) of v-B_2O_3 obtained in 90° scattering. For polar vibrations, only the TO component is active in HRS for this scattering geometry [10]. The eigenvectors of the modes labeled **1** to **5** are shown at the top of figure 1 [16]. The BP (mode **1**) corresponds to librational motions of rigid ESUs. In a connected network, like v-B_2O_3, each such mode involves several units and librations necessarily couple to translations. Modes **2**, **3**, and **5** correspond to motions of oxygen and boron atoms in opposite directions, perpendicular (**2** and **3**) or parallel (**5**) to the ESU plane. These vibrations modulate the dipole moment and they are thus active in IR. Indeed, their frequency matches the position of the IR bands, which are represented by vertical lines in figure 1(a). The component **4** at 808 cm^{-1} is associated with the local symmetric stretch, or breathing mode, A_1' of the boroxols [19]. It completely dominates the RS spectrum (figure 1(b)). In this vibration, only oxygen atoms are involved and their motion does not modulate the dipole moment. In agreement with (2), this mode is active both in RS and HRS and inactive in IR. Its experimental HRS depolarization ratio, $\rho_{\mathrm{HRS}} = I_{\mathrm{VH}}/I_{\mathrm{VV}}$, perfectly matches the expected value, 2/3 [20].

For the boson peak **1**, one cannot exclude a weak IR activity on the basis of the available information. As shown in figure 1, the boson peak is active both in RS and HRS. Although these two spectra are not identical, one should remark that the boson peak signature is very similar in both spectroscopies. The HRS boson peak has been associated with the E'' librational motions of rigid ESUs [15, 16]. Librations are external motions of coupled ESUs. The fact that adjacent units move in opposite directions can lead to constructive coherent effects in HRS and destructive ones in RS [15]. This can explain the relatively intense boson peak observed in HRS.

Another coherent effect produces the strong polar doublet around 700 cm^{-1}. Here the coherence is not of mechanical but rather of electromechanical origin. These modes are associated with A_2''-symmetry vibrations corresponding to out-of-plane

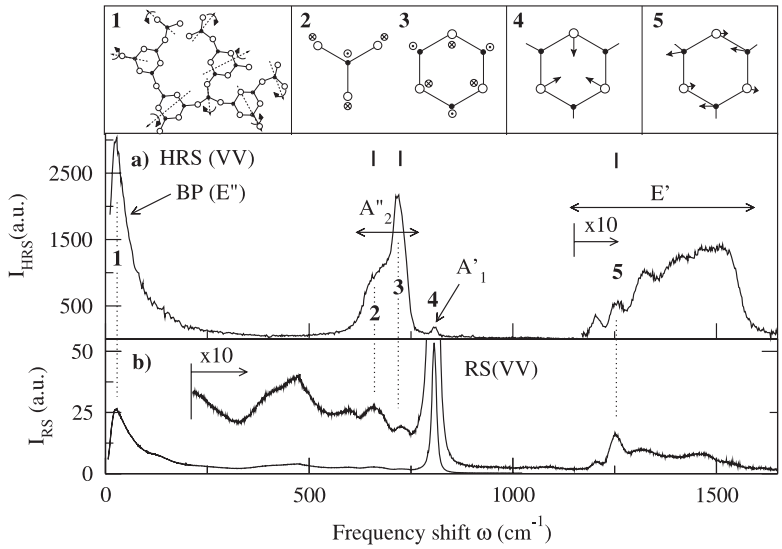

Figure 1. Spectroscopy of v-B_2O_3 in 90° scattering: (a) hyper-Raman VV spectrum; (b) Raman VV spectrum from the same sample. The frequencies ω are expressed in wavenumbers, $\omega/2\pi c$. The top panels illustrate the eigenvectors of the modes labeled **1**–**5**.

motions of oxygen and boron ions in antiphase (see the eigenvectors in figure 1). Motions in triangles give the broad band **2** centered around 665 cm^{-1}, while the rings, whose structure is very regular, give the intense narrow line **3** at 720 cm^{-1}. These modes are expected to be inactive in RS (equation (2)). However, one observes a weak intensity in figure 1(b). This could result from a small departure from planarity of the ESUs, as this very effectively lifts the RS selection rules. In addition, several ESUs being connected, internal modes involving the motion of connecting atoms can always contain a small number of external displacements which are Raman active.

The origin of the multicomponent structure above 1200 cm^{-1} is more involved. A complete description would certainly require the help of simulations. However, our analysis in [16] revealed that these polar modes are mainly associated with E′-symmetry vibrations. They correspond to in-plane motions of oxygen and boron atoms in triangles and rings. The weak HRS line **5** at 1265 cm^{-1} gives an intense IR absorption band. It corresponds to the motions inducing the largest dipole moment fluctuations. This occurs in boroxols and it was observed from isotopic substitution [19] that the mode involves both boron and oxygen atoms, moving as tentatively sketched in figure 1.

4. Hyper-Raman scattering in lithium borate glasses

The addition of lithium oxide to boron oxide produces a major structural change owing to the formation of negative $BO^-_{4/2}$ tetrahedra. These are charge compensated by Li^+ ions [21]. For a composition B_2O_3:yLi_2O, or $(1-x)B_2O_3$:xLi_2O, the maximum fraction of four-coordinated borons that can thereby be produced is $N_4 = y = x/(1-x)$. This is close to the observed value in lithium tetraborate ($y = 1/4$), whereas $N_4 \simeq 0.4$ in the diborate glass ($y = 1/2$) as known from NMR results [22]. When $N_4 < y$, the remaining Li^+ ions can be charge compensated by negative non-bridging oxygens. The random formation of tetrahedra very effectively reduces the number of adjacent BO_3 triangles and thus it dramatically depresses the number of boroxols. It is of interest to note that in crystalline lithium diborate, $Li_2B_4O_7$, N_4 is exactly 0.5, half of the borons forming tetrahedra and the other half forming BO_3 triangles [23]. HRS spectra were obtained for $y = 1/4$ and $1/2$. These samples were kindly provided by Dr A Matic from Chalmers University of Technology, Göteborg, Sweden.

In lithium borate glasses one expects three types of randomly connected basic ESUs: the triangles, the boroxol rings at low Li concentration, and the tetrahedra. This considerably complicates the IR and RS spectra. These ESUs can form a wide variety of larger units depending on the Li concentration [24]. It is known that these have specific vibrations which are different from just the sum of vibrations of the constitutive ESUs. A good example is the triborate ion $B_3O_5^-$, which can be viewed as two triangles bonded to one tetrahedron and which forms the basic unit of crystalline lithium triborate LiB_3O_5 [25]. However, in the glass so many different larger units coexist that we rather view their vibrations as contributions to the important broadening of the basic ESU bands. Further, the HRS experiments revealed that fine features of the v-B_2O_3 spectra rather wash out upon introduction of Li. Hence, it will not be helpful here to invoke specific modes of larger units, and our discussion will be based on the simplest ESUs. Figure 2 compares the HRS depolarized spectra (VH) of the three samples observed in 90° scattering. Similarly to pure boron oxide, the HRS spectra of lithium borates are very different from the RS and IR ones [26]. A main difference is that fewer distinct modes superimpose in the spectra. Moreover, one can easily separate LO and TO contributions in HRS. Following the selection rules for 90° scattering [10], the intensities of polar modes are given by $I_{\mathrm{HRS,TO}} \propto \frac{1}{2}a^2_{\mathrm{TO}}$ and $I_{\mathrm{HRS,LO}} \propto \frac{1}{2}a^2_{\mathrm{LO}}$ in VH polarization. In VV polarization, they are $I_{\mathrm{HRS,TO}} \propto 9a^2_{\mathrm{TO}}$ and $I_{\mathrm{HRS,LO}} = 0$.

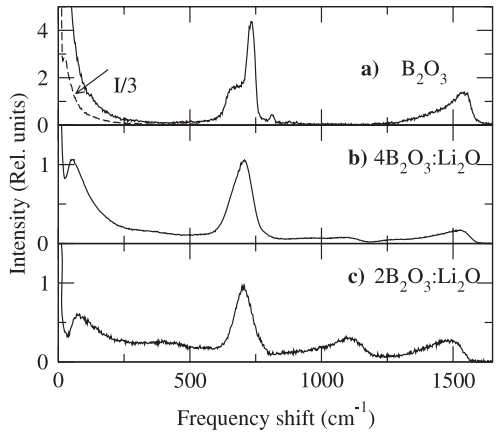

Figure 2. A comparison of HRS spectra obtained in 90° scattering for VH polarization.

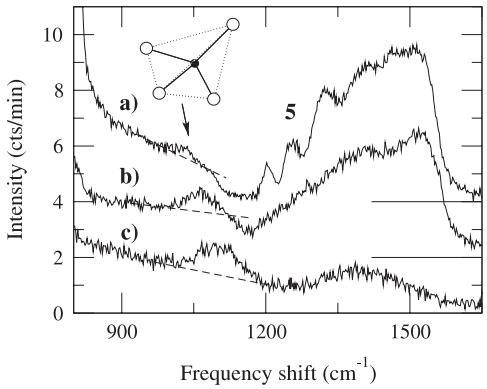

Figure 3. HRS VV spectra from the high frequency bands in 90° scattering. For clarity, the spectra of v-B_2O_3 (a) and $4B_2O_3$:Li_2O (b) have been vertically translated by 4 and 2, respectively, while (c) corresponds to $2B_2O_3$:Li_2O. One recognizes the F_2-symmetry mode of BO_4 tetrahedra at ∼1100 cm^{-1} and the E′-symmetry multiband above 1200 cm^{-1}. The dashed lines roughly estimate the background in the region of the BO_4 vibrations (see text).

The coupling coefficients a_{TO} and a_{LO} are different for each type of modes, and usually $a_{LO} \gg a_{TO}$ owing to the electro-optic coupling of the LO modes with the internal electric field. Hence, the LO components dominate the VH hyper-Raman spectra in figure 2[1].

The presence of a new type of ESU in lithium borates is clearly evidenced by a new broad band around 1100 cm^{-1} whose intensity increases together with the Li concentration. Its HRS depolarization ratio is larger than unity, while one expects $\rho_{HRS} \leqslant 2/3$ for non-polar modes [20]. This establishes that this band is the LO component of a polar mode. Therefore, it should be active in IR absorption. Indeed, this band peaks in a frequency region where stretching modes of four-coordinated borons dominate as well as other vibrations arising from larger structures involving BO_4 tetrahedra [24]. Interestingly, the HRS spectra of silica and sodium silicate glasses also exhibit a structure in this frequency region [12]. We associate the HRS band around 1100 cm^{-1} in the lithium borates with stretching motions of BO_4 tetrahedra. This is confirmed by the RS analysis of crystalline $Li_2B_4O_7$, in which the 1143 cm^{-1} mode is assigned to ν_3 tetrahedral distortions [27]. Presumably, the variety of surroundings does broaden this band in the glass. Within the point group T_d of tetrahedral molecules, this mode corresponds to F_2-symmetry vibrations [28–30], active in all three spectroscopies, IR, RS, and HRS. In Raman, this mode is weakly seen only in the diborate sample [12], suggesting a small light-to-vibration coupling coefficient.

Figure 3 zooms in on the high frequency region of the *polarized* HRS spectra (VV). As already mentioned, only the TO components of the polar vibrations are active in this geometry. One can try relating the strength of the BO_4 stretching modes at ∼1100 cm^{-1} to the number of tetrahedra in the structure. This is done using the TO spectra rather than the LO ones, as in the former the intensities are not affected by the electro-optic coupling term, which is likely to depend on the glass composition. Indeed, the strength of the LO component increases nearly tenfold between our two lithium borate samples, which is much larger than either the increase in the Li concentration or in the fraction of BO_4 tetrahedra. The background scattering in v-B_2O_3 clearly suggests a Reststrahlen gap between ∼1110 and ∼1190 cm^{-1}. Unfortunately, the TO component of the BO_4 stretching mode peaks on the edge of this vibrational gap and the shape of the background signal in this region is thus hard to determine. The low frequency side of this gap is tentatively represented by dashed lines in figure 3. We estimate that the relative area of the peak in tetraborate is 1.5–2 times smaller than in diborate. This is in qualitative agreement with early work, which showed that the fraction N_4 of four-coordinated borons increases from $N_4 \simeq 0.22$ to $N_4 \simeq 0.40$ from $x = 0.2$ to 0.33 [21]. The proportionality of the signal to N_4 suggests that at these concentrations the BO_4 stretching vibrations are sufficiently local to scatter incoherently. One knows from numerical simulations that the BO_4 tetrahedra are relatively well defined in lithium borates, with an average O–B–O angle of ∼109.5° ± 7° [31]. This value is similar to that of the O–Si–O angle in v-SiO_2 and it does not significantly depend on the alkali concentration. The increase in the inhomogeneous linewidth of the HRS stretching band must arise from the broad distribution of local BO_4 surroundings. In sodium–silicate glasses the effect of sodium is to disrupt the SiO_2 network, and indeed one observes a softening of the high frequency SiO_4-stretching vibrations [12]. The inverse occurs in lithium borates. This suggests that the frequency dependence of this mode is directly related to the connectivity of the network. A quantitative description of the above observations would require further experiments and simulations. It is finally interesting to remark that a weak peak at ∼1050 cm^{-1} is already seen in our 'pure' B_2O_3 sample. This suggests that this sample does contain some BO_4 tetrahedra, possibly owing to cationic impurities.

The destruction of boroxol rings with lithium substitution not only generates a new band in the HRS spectrum, but it also strongly transforms existing ones. For example, narrow

[1] However, the best scattering geometry for the observation of pure LO modes is near forward scattering, using a suitable mask for the collection of the scattered light [16].

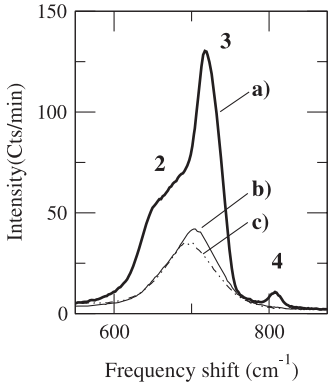

Figure 4. HRS VV spectra of lithium borate glasses in the frequency region between 550 and 900 cm^{-1}. The labels (a), (b), and (c) are the same as in figure 3. The numbers **2–4** refer to the vibrations represented in figure 1.

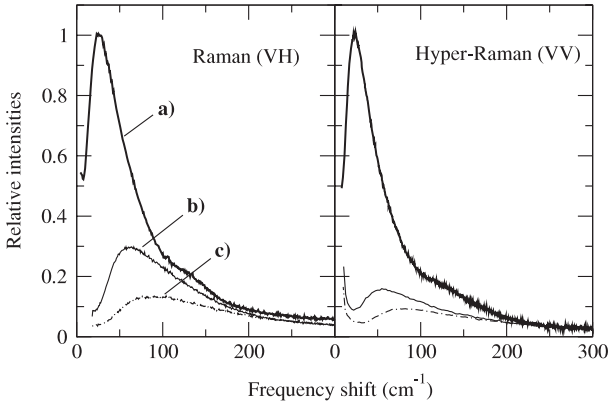

Figure 5. RS and HRS boson peaks of the three samples in approximative relative units. VH polarization is used for the RS spectra in order to minimize the contributions of other low frequency modes. Similarly, the VV spectra are used in HRS in the 90° scattering geometry to avoid the LO contributions.

lines at 1210, 1265, and 1325 cm^{-1} in figure 3 disappear in lithium borates, suggesting that they all originate in boroxol vibrations. In addition, the A_2'' doublet centered around 700 cm^{-1} transforms into a single peak in the lithium borates, as shown in figure 4. Here, the high frequency narrow component **3** at 720 cm^{-1} associated with motions in boroxols disappears in the binary glasses, and only the A_2''-symmetry modes **2** arising from the BO_3 triangles remain. Owing to the proximity of these two bands, it is difficult to extract from them information on the relative amount of boroxols in the glasses. This is rather done with the intense RS line **4** produced by the breathing motions of oxygens in boroxols [26]. As observed in figures 1 and 3, this breathing mode is also active in HRS but with a very weak intensity. One finds that the boroxol concentration in tetraborate is reduced to $\simeq$24% of that in v-B_2O_3. This means that in tetraborate there are about five triangles and eight tetrahedra for one boroxol. Practically no boroxol remains in diborate.

A broad band centered around 450 cm^{-1} also appears in the lithium borate glasses (figure 2). It gives an intense and asymmetric signature that decreases to very low frequency in IR [24]. These low frequency motions have been assigned to vibrations of the Li–O bonds on various anionic sites. The band is weak in HRS for 90° scattering and masked by the wing of the strong lower frequency boson peak. The analysis of this mode would be easier in near forward scattering, as one expects then an 18 times stronger LO intensity, while the HRS efficiency of the boson peak should remain unchanged [16]. The above completes our discussion of modes that are *internal* to the ESUs.

5. The boson peak of lithium borate glasses

Raman scattering by the boson peak has been observed in a large number of alkali borates as a function of their composition [32]. This was repeated recently for more Li concentrations [33]. Raman and hyper-Raman boson peak spectra obtained on our samples are illustrated in figure 5. The observed variations with composition are qualitatively similar in both spectroscopies. The main features are summarized in table 1. The frequency position of the boson peak maximum, Ω_{BP}, shifts rapidly up with increasing Li content. The relative scattering intensities also dramatically decrease with concentration y in both spectroscopies. The decrease of the HRS intensities, I^{HRS}, is faster than that of the RS intensities, I^{RS}, as seen in figure 5 and in table 1.

Table 1. Concentration dependence of the boson peak positions and relative peak heights extracted from figure 5. The longitudinal acoustic velocities v_L are from [32].

y	Ω_{BP}^{RS} (cm^{-1})	Ω_{BP}^{HRS} (cm^{-1})	I_{VH}^{RS}	I_{VV}^{HRS}	v_L ($m\ s^{-1}$)
0	25.7 ± 0.2	23.5 ± 0.5	1	1	3550
0.25	62 ± 1	55 ± 1	0.29	0.16	5800
0.50	90 ± 1	79 ± 1	0.13	0.08	6820

The boson peak of glasses presumably arises from *external* rigid motions of ESUs. This was shown to be the case for silica [13, 34] and for boron oxide [15]. In crystals, these external motions lead to rather sharp low frequency spectral lines, whereas in glasses, owing to their disorder, one observes a broad distribution of quasi-local vibrations (QLVs) in the sense of Lifshitz [35]. This crucial difference becomes here obvious in comparing the Raman spectrum of crystalline $Li_2B_4O_7$ [27] to that of glassy $Li_20{:}2B_2O_3$ shown in figure 5. The precise model leading to the universal occurrence and spectral shape of boson peaks in dielectric glasses is still being strongly debated. A rather successful proposal is that the QLVs elastically interact with each other and that this mediates a universal reconstruction of their density of vibrational states $g_0(\omega)$ into a $g(\omega)$ that exhibits a boson peak when plotted as $g(\omega)/\omega^2$ versus ω [36, 37]. It is important to notice that rigid motions of ESUs involve both librations and translations. Both types of motion can contribute to the scattering strength, and in network glasses these motions must generally be strongly coupled. HRS mainly sees the librational part of the modes, as the coupling-to-light coefficient for translations is usually very weak in HRS [38], as opposed to RS, to which translations always contribute.

The data will now be discussed within the boson peak model based on the elastic interactions of QLVs [36].

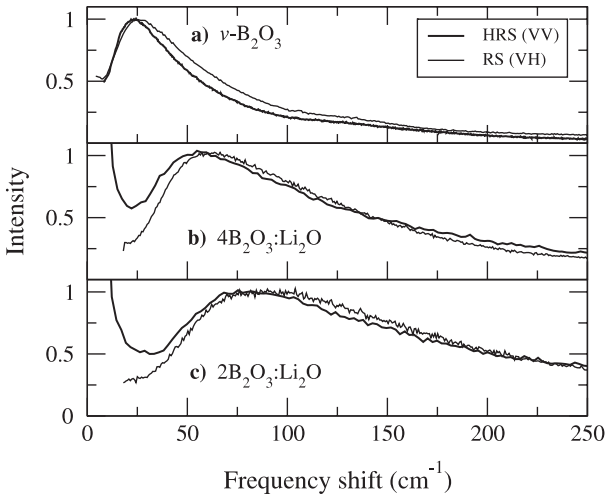

Figure 6. '—' RS (VH) and '——' HRS (VV) boson peaks in lithium borate glasses normalized to their maxima. The spectra are those shown in figure 5.

Assuming that one could compare glasses having different sound velocities but the *same* bare density $g_0(\omega)$, the effect of the elastic interaction is that Ω_{BP} should scale with a typical high frequency sound velocity, v, while the height of $g(\omega)/\omega^2$ should scale as $1/v^3$. The values of the longitudinal acoustic velocities v_L, taken from [32], are also listed in table 1. The transverse velocities, v_T, are such that $v_T/v_L \simeq 0.57$ for all compositions [32]. Hence, one can simply use v_L as a typical v in the above considerations. One notices in table 1 that the boson peak positions vary much faster with y than v_L does. One nearly finds $\Omega_{BP} \propto v_L^2$. This shows that the frequency shifts cannot solely be explained by a local hardening of the glass network. Thus the nature of the QLVs producing the boson peak must also evolve with the composition y, of course in relation to the considerable structural changes. In fact, the librations of tetrahedra are expected to be on average faster than these of boroxols, for two reasons: they have a smaller moment of inertia and they are more bonded within the network. We also notice in table 1 and figure 6 that a slight shift of Ω_{BP} towards lower frequencies seems to systematically occur in HRS compared to RS. This was interpreted in [15] as arising from the coherent motion of neighboring ESUs. The hyper-Raman efficiency is enhanced by correlated ESUs, which down-shifts Ω_{BP}, as on average larger entities should be more enhanced but also librate at lower frequencies.

Consider now the decrease of the scattering intensity with increasing y. Remarkably, one finds from the values in table 1 that $I_{VH}^{RS} \times v_L^3$ is nearly constant. This seems to imply that the network hardening is sufficient to explain the evolution with y of the RS intensity. Measurements of the specific heat C_p [39] of boron oxide and lithium diborate indicate that their excess in C_p/T^3 scales with their Debye values C_D/T^3. The latter being proportional to $1/v_L^3$, the above result simply implies that the coupling to light of the QLVs does not vary much with y. This could possibly result from the averaging of the many contributions, librational and translational, to the RS signal. On the other hand, one observes in table 1 that I_{VV}^{HRS} decreases twice as much as I_{VH}^{RS} from $y = 0$ to $1/4$. This could reflect a decrease in the coherent enhancement of the HRS boson peak signal [15]. Such a decrease of coherence can easily be produced by the mixing in of Li^+ ions and of ESUs of different symmetries.

6. Conclusion

The HRS spectra of borate glasses have been analyzed using a rather simple structural model that takes into account the symmetry of the basic ESUs. This model accounts for the main HRS bands in v-B_2O_3 and in lithium doped borate glasses. The appearance of $BO_{4/2}^-$ tetrahedra and the disappearance of boroxols with increasing Li^+ content is reflected in the HRS spectra. In particular, the TO–LO line around 1100 cm^{-1} which appears in lithium borates can be assigned to F_2-symmetry stretching motions of BO_4 tetrahedra. The integrated HRS intensity of this TO component is proportional to the number of tetrahedra in the glass. Also, the modification of the 700 cm^{-1} band reflects the disappearance of boroxols observed on their A_2'' vibrations. Concerning the boson peak, the most dramatic effect is the fast decrease of the scattering intensity with increasing Li^+ content. This can be accounted for to a large extent by a hardening of the network. However, the strong shift of the boson peak position presumably reflects an overall up-shift of QLV frequencies, owing to the faster rigid motions of $BO_{4/2}^-$ tetrahedra.

Acknowledgments

The authors express their appreciation to Saint-Gobain Recherche, and in particular to Dr M-H Chopinet and Dr P Lambremont, for their guidance in glass preparation and the use of their facility. Thanks are also addressed to Dr A Matic from Chalmers University for providing samples of lithium borates.

References

[1] Galeener F L 1982 *Solid State Commun.* **44** 1037
[2] Giacomazzi L, Umari P and Pasquarello A 2005 *Phys. Rev. Lett.* **95** 075505
[3] Burgin J, Guillon C, Langot P, Vallée F and Hehlen B 2006 *Appl. Phys. Lett.* **89** 251913
[4] Mozzi R L and Warren B E 1970 *J. Appl. Crystallogr.* **3** 251
[5] Jellisson G E, Panek L W, Bray P J and Rouse G B 1977 *J. Chem. Phys.* **66** 802
[6] Galeener F L, Lucovsky G and Mikkelsen J C Jr 1980 *Phys. Rev.* B **22** 3983
[7] Umari P, Gonze X and Pasquarello A 2003 *Phys. Rev. Lett.* **90** 027401
[8] Zwanziger J W 2005 *Solid State Nucl. Magn. Reson.* **27** 5
[9] Umari P and Pasquarello A 2005 *Phys. Rev. Lett.* **95** 137401
[10] Denisov V N, Mavrin B N and Podobedov V B 1987 *Phys. Rep.* **151** 1
[11] Guillon C, Burgin J, Langot P, Vallée F and Hehlen B 2005 *Appl. Phys. Lett.* **86** 081909
[12] Simon G 2007 *Doctoral Thesis* University of Montpellier II, France
[13] Hehlen B, Courtens E, Vacher R, Yamanaka A, Kataoka M and Inoue K 2000 *Phys. Rev. Lett.* **84** 5355

[14] Hehlen B, Courtens E, Yamanaka A and Inoue K 2002 *J. Non-Cryst. Solids* **307** 87
[15] Simon G, Hehlen B, Courtens E, Longueteau E and Vacher R 2006 *Phys. Rev. Lett.* **96** 105502
[16] Simon G, Hehlen B, Vacher R and Courtens E 2007 *Phys. Rev.* B **76** 054210
[17] Cyvin S J, Rauch J E and Decius J C 1965 *J. Chem. Phys.* **43** 4083
[18] Ramos M A, Moreno J A, Viera S, Prieto C and Fernandez J F 1997 *J. Non-Cryst. Solids* **221** 170
[19] Windisch C F Jr and Risen W M Jr 1982 *J. Non-Cryst. Solids* **48** 307
[20] Bersohn R, Pao Y-H and Frisch H L 1966 *J. Chem. Phys.* **45** 3184
[21] Bray P J and O'Keefe J G 1963 *Phys. Chem. Glasses* **4** 37
[22] Zhong J and Bray P J 1989 *J. Non-Cryst. Solids* **111** 67
[23] Krogh-Moe J 1968 *Acta Crystallogr.* B **24** 179
[24] Kamitsos E I, Patsis A P, Karakassides M A and Chryssikos G D 1990 *J. Non-Cryst. Solids* **126** 52
[25] Xiong G, Lan G, Wang H and Huang C 1993 *J. Raman Spectrosc.* **24** 785
[26] Kamitsos E I, Karakassides M A and Chryssikos G D 1987 *Phys. Chem. Glasses* **28** 203
[27] Paul G L and Taylor W 1982 *J. Phys. C: Solid State Phys.* **15** 1753
[28] Wilson M, Madden P A, Hemmati M and Angel C A 1996 *Phys. Rev. Lett.* **77** 4023
[29] Taraskin S N and Elliott S R 1997 *Phys. Rev.* B **56** 8605
[30] Sarthein J, Pasquarello A and Car R 1997 *Science* **275** 1925
[31] Varsamis C-P E, Verigi A and Kamitsos E I 2002 *Phys. Rev.* B **65** 104203
[32] Lorösch J, Couzi M, Pelous J, Vacher R and Levasseur A 1984 *J. Non-Cryst. Solids* **69** 1
[33] Kojima S, Novikov V N and Kodama M 2000 *J. Chem. Phys.* **113** 6344
[34] Buchenau U, Prager M, Nücker N, Dianoux A J, Ahmad N and Phillips W A 1986 *Phys. Rev.* B **34** 5665
[35] Lifshitz I M 1943 *J. Phys. (USSR)* **7** 86
Lifshitz I M 1943 *J. Phys. (USSR)* **7** 215
Lifshitz I M 1944 *J. Phys. (USSR)* **8** 82
[36] Gurevich V L, Parshin D A and Schober H R 2003 *Phys. Rev.* B **67** 094203
[37] Parshin D A, Schober H R and Gurevich V L 2007 *Phys. Rev.* B **76** 064206
[38] See e.g. Shelton D P 2002 *J. Chem. Phys.* **117** 9374
[39] Carini G 2006 private communication